Received: 25 June 2020 | Revised: 24 October 2020 | Accepted: 12 November 2020

DOI: 10.1002/hbm.25295

RESEARCH ARTICLE

WILEY

Neurophysiological mechanisms underlying motor feature binding processes and representations

Adam Takacs[1] | Annet Bluschke[1] | Maximilian Kleimaker[2,3] | Alexander Münchau[2] | Christian Beste[1]

[1]Cognitive Neurophysiology, Department of Child and Adolescent Psychiatry, Faculty of Medicine, TU Dresden, Dresden, Germany

[2]Institute of Systems Motor Science, University of Lübeck, Lübeck, Germany

[3]Department of Neurology, University of Lübeck, Lübeck, Germany

Correspondence
Christian Beste, Cognitive Neurophysiology, Department of Child and Adolescent Psychiatry, Faculty of Medicine of the TU Dresden, Schubertstrasse 42, D-01309 Dresden, Germany.
Email: christian.beste@ukdd.de

Funding information
Deutsche Forschungsgemeinschaft, Grant/Award Number: FOR 2698

Abstract

Coherent, voluntary action requires an integrated representation of these actions and their defining features. Although theories delineate how action integration requiring binding between different action features may be accomplished, the underlying neurophysiological mechanisms are largely elusive. The present study examined the neurophysiological mechanisms underlying binding processes in actions. To this end, we conducted EEG recordings and applied standard event-related potential analyses, temporal EEG signal decomposition and multivariate pattern analyses (MVPA). According to the code occupation account, an overlap between a planned and a to-be-performed action impairs performance. The level, to which performance is attenuated depends on the strength of binding of action features. This binding process then determines the representation of them, the so-called action files. We show that code occupation and bindings between action features specifically modulate processes preceding motor execution as showed by the stimulus-locked lateralized readiness potential (LRP). Conversely, motor execution processes reflected by the response-locked LRP were not modulated by action file binding. The temporal decomposition of the EEG signal, further distinguished between action file related processes: the planned response determining code occupation was reflected in general (voluntary) response selection but not in involuntary (response priming-related) activation. Moreover, MVPA on temporally decomposed neural signals indicated that action files are represented as a continuous chain of activations. Within this chain, inhibitory and response re-activation patterns can be distinguished. Taken together, the neurophysiological correlates of action file binding suggest that parallel, stimulus- and response-related pre-motor processes are responsible for the code occupation in the human motor system.

KEYWORDS

EEG, motor representations, motor system, MVPA, neurophysiology, theory of event coding

Alexander Münchau and Christian Beste shared senior authorship.

1 | INTRODUCTION

Coherent, voluntary action requires a clear representation (plan) of these actions in the brain. In daily life, this is particularly relevant since most goal-directed behavior consists of multiple components and requires a concatenation of different actions to achieve a goal (Dippel & Beste, 2015; Duncan, 2010; Stoet & Hommel, 1999). Moreover, these different components are defined by multiple features such as which effector is to be used with a specific speed or force at a specific time. This feature specification is then also likely to require multiple brain systems. What follows is that planning voluntary action requires intricate coordination and integration of information. This integration and specification of actions, similar to the representation of perceptions, faces so-called binding problems (Hommel, 2004; Stoet & Hommel, 1999): that is, how are different features constituting an action related and connected to each other?

A prominent theory addressing how integration and binding during action (planning) may work on a conceptual level, is the Theory of Event Coding (TEC) (Hommel, 2009; Hommel, Müsseler, Aschersleben, & Prinz, 2001). Generally, TEC is concerned with the question of how different features constituting object representations as well as actions are integrated. Central to TEC is that it assumes three types of "files": an "object file," an "event file" and an "action file." An object file is constituted by the features of perceived stimuli (Treisman, 1996; Treisman & Kahneman, 1984), an action file by the features defining a response (Hommel et al., 2001). An "event file" in turn represents the inter-relation of object and action files; that is, how specific stimulus features are related to specific action features (Hommel, 2004). Several lines of evidence have corroborated the concept of bindings between stimulus features and between stimulus and response features (Colzato, Warrens, & Hommel, 2006; Henson, Eckstein, Waszak, Frings, & Horner, 2014; Moeller, Pfister, Kunde, & Frings, 2019). Similarly, studies have also delineated the associated neurophysiological and functional neuroanatomical correlates (Keizer, Verment, & Hommel, 2010; Kühn, Keizer, Colzato, Rombouts, & Hommel, 2011; Opitz, Beste, & Stock, 2020; Petruo, Stock, Münchau, & Beste, 2016; Takacs, Mückschel, Roessner, & Beste, 2020). However, astonishingly little is known about the neurophysiological (electrophysiological) implementation of action file bindings, that is, how action-related features are integrated. Similarly, it is elusive how the representational content of action files is reflected on a neurophysiological level. The current study intends to close these gaps in knowledge.

Twenty years ago, Stoet and Hommel (1999) developed an experimental approach to examine feature bindings in action files. The approach is based on a code-occupation logic. According to this logic, action activation is more than just activating various features defining an action, that is, which effector is to be used with a specific speed or force at a specific time. Rather, it is necessary to integrate these different codes belonging to an action. For instance, a simple action, like opening the fridge requires the integration of the feature codes of the left or right arm, the distance towards the fridge, the moderate speed of the action, and the power of the grabbing move, and so forth. Importantly, this integration of features defining an action involves what the authors call "code occupation" (Stoet & Hommel, 1999). For example, when one plans to carry out a right arm movement, all features related to/defining this planned movement become activated—including the feature "*right*." The important point is that until this planned "*right*" arm movement has not been executed, the "*right*" code is reserved (occupied) for that specific movement. This preoccupation of code makes it difficult to plan/execute another action that also uses the "*right*" code. Such an overlap between a planned and a to-be-performed action impairs performance. The degree, to which performance is impaired depends on the strength of binding (integration) of features (Colzato et al., 2006; Stoet & Hommel, 1999). The experimental approach to examine action file coding processes thus employs a design, in which an action (A) is planned, but its execution has to be postponed until another action (B) was planned and performed. This ABBA response execution approach measures the effect of an already formed action plan on the efficiency to plan and execute another action/movement. It has been shown that performance is better, that is, reaction times (RTs) are shorter, when there is no feature overlap between the A and the B motor response—that is when there is no code-occupation (Colzato et al., 2006; Stoet & Hommel, 1999).

From a neurophysiological point of view, and using EEG methods, movement-related processes can be examined using the lateralized readiness potential (LRP) (Coles, 1989; Gratton, Coles, Sirevaag, Eriksen, & Donchin, 1988)—an index of response activation and preparation (Coles, 1989; de Jong, Wierda, Mulder, & Mulder, 1988) generated in motor cortical areas (Leuthold & Jentzsch, 2001). The LRP can be formed in two ways—stimulus-locked (s-LRP) and response locked (r-LRP). The s-LRP is supposed to be a measure of processes preceding motor execution, that is, pre-motor processes, the r-LRP reflects processes related to the subsequent motor execution (Beste et al., 2009; Coles, 1989; Masaki, Wild-wall, Sangals, & Sommer, 2004; Osman, Moore, & Ulrich, 1995; van der Lubbe, Jaśkowski, Wauschkuhn, & Verleger, 2001; Wild-Wall, Sangals, Sommer, & Leuthold, 2003). Code-occupation processes reflecting the integration of different action-related features precede the overt motor response. Therefore, we hypothesize that particularly the s-LRP is modulated by experimental variations. In other words, the s-LRP is hypothesized to reflect the impact of an already formed action plan "A" on the efficiency to plan action "B". More specifically, we hypothesize that (a) the s-LRP will be larger and (b) its onset earlier when there is no code-occupation between actions A and B, compared to conditions when features are shared between actions A and B. Previous findings suggest that when pre-motor inhibition is demanding, a correct negative LRP deflection is preceded by a short-lasting positive deflection that indicates the activation of the wrong response (Beste, Baune, Falkenstein, & Konrad, 2010; Beste, Saft, Andrich, Gold, & Falkenstein, 2008; Bryce, Szűcs, Soltész, & Whitebread, 2011; Falkenstein, Willemssen, Hohnsbein, & Hielscher, 2006; Gratton, Coles, & Donchin, 1992; Stürmer, Leuthold, Soetens, Schröter, & Sommer, 2002; Zhang et al., 2018)—in our case

the response A when there is action file feature overlap between response A and B. However, it cannot be excluded that also motor execution processes per se are modulated by the experimental variations. Therefore, we also explore, how far the r-LRP is modulated by experimental variations.

Besides, it is important to mention that previous studies examining the neurophysiology of binding processes within the TEC-framework obtained most robust effects after applying temporal signal decomposition methods (Opitz et al., 2020; Takacs, Mückschel, et al., 2020), that is, residue iteration decomposition (RIDE) (Ouyang, Sommer, & Zhou, 2015). Applying RIDE, stimulus-locked data is decomposed into three "clusters", each reflecting dissociable processes. The "S-cluster" reflects stimulus-triggered processes, the "R-cluster" processes related to movement execution and the "C-cluster" processes between stimulus evaluation and responding (Ouyang et al., 2015; Ouyang, Herzmann, Zhou, & Sommer, 2011). Previous studies of event file coding emphasized the role of the C-cluster (Kleimaker et al., 2020; Opitz et al., 2020; Takacs, Mückschel, et al., 2020). Translational processes between stimulus and response codes were detectable in the C-cluster signal, but not in the S-cluster and R-cluster data (Kleimaker et al., 2020; Opitz et al., 2020; Takacs, Mückschel, et al., 2020). Moreover, event file binding related modulations in the P3 ERP component were evident in the C-cluster as opposed to the undecomposed EEG (Kleimaker et al., 2020; Opitz et al., 2020), or the P3 effect was stronger in the C-cluster than in the undecomposed EEG as reflected by effect sizes and confidence intervals (Takacs, Mückschel, et al., 2020). Thus, in case of event files, modulations of the P3 in the C-cluster seems to be the most important neurophysiological marker. However, in case of action files, binding does not occur between stimulus and response, but between response codes (Stoet & Hommel, 1999). Therefore, motor components, such as the LRP, are better suited to study the neurophysiology of action files. Crucially, RIDE has also been applied to s-LRPs in tasks where different (incompatible) actions are activated (Stürmer, Ouyang, Zhou, Boldt, & Sommer, 2013). Stürmer et al. (2013) showed that RIDE applied to s-LRPs allows for dissociation of response activation effects due to priming from processes of voluntary response selection. This is also relevant for the action file paradigm since actions A and B can show feature overlaps making it difficult to select the required response B. Indeed, Stürmer et al. (2013) showed that particularly the S-cluster and the R-cluster reflect processes of response priming and selection, respectively. In contrast, the C-cluster LRP did not show any modulation related to response preparation processes. Moreover, as action files should reflect processes at the response code level, it is expected that the R-cluster will primarily show the action file binding effect. Therefore, we hypothesize that particularly the R-cluster s-LRP is modulated by experimental variations of action file binding as opposed to the C-cluster which is implicated in event files.

Although the above-mentioned analyses will provide insights into neurophysiological subprocesses involved in action file binding effects, these analyses do not yield information with respect to the neurophysiology associated with the stability of action file representations. To answer this question, multivariate pattern analysis (MVPA) applied to EEG (King & Dehaene, 2014) is useful since it decodes the representational difference between experimental conditions based on the observed neural patterns (Carlson, Grootswagers, & Robinson, 2019; Fahrenfort, van Driel, van Gaal, & Olivers, 2018). Importantly, temporal generalization analyses can provide insights into the stability of mental representations over time (Fahrenfort et al., 2018; Grootswagers, Wardle, & Carlson, 2016; King & Dehaene, 2014), that is, it is possible to examine when and for how long action file information is detectable in neural activity. Since MVPA is, in theory, applicable to a variety of EEG data types (time domain, time-frequency domain, etc.) (Carlson et al., 2019), we use the undecomposed and RIDE-decomposed data as a basis for the MVPA analysis. A similar approach was used recently for studying event files (Takacs et al., 2020). Using MVPA, different temporal generalization patterns across time can be distinguished (King & Dehaene, 2014) indicating, for instance, a chaining of processes (i.e., diagonal-shaped decoding performance) or a continuous activation of representations (i.e., diagonal and off-diagonal decoding performance). A continuous activation indicates a single representational activation, which can be fading (jittered activity pattern) or strengthening (ramped activity pattern) over time. Conversely, a chain-like activation indicates multiple components; each of them generalizes for a brief time only (King & Dehaene, 2014). A previous study suggested that generalization of event files can be detected predominantly in the C-cluster data (Takacs, Zink, et al., 2020). During event file coding, a sustained neural activity was shown in the C-cluster. The smoothing and temporally jittered nature of the activation suggested a single, gradually developing representation behind the event files. The S-cluster showed a similar temporal generalization pattern, albeit with smaller activity. However, the R-cluster painted a different picture. Namely, a ramping activity characterized the whole trial length, except for a non-significant activity corresponding to the time windows of the main activations in the C- and S-clusters. This mirror-reversed pattern distinguished the representation of motor execution processes (R-cluster) from the stimulus-related, and stimulus–response translational representation (S- and C-cluster). However, the question remained, what type of neural activity emerges from binding of motor or action-related features. We assume that binding processes in action files will be evident for several hundred milliseconds and that diagonally-shaped as well as off-diagonal decoding performance will be present. The latter is hypothesized to be evident due to the structure and logic of the experimental paradigm, in which a chain of different actions has to be planned and performed.

Taken together, this study uses a multi-methodological approach: After analyzing standard s-LRP and r-LRPs, signal decomposition (i.e., RIDE) is used to examined s-LRP processes in more detail before MVPA is applied to examine the stability of neural processes involved in action file coding.

2 | MATERIALS AND METHODS

2.1 | Participants and power considerations

A sample of N = 30 (12 male and 18 female, M_{age} = 30.4, SD_{age} = 4.2 years) healthy adults with no neurological or psychiatric disorder was recruited from the university's voluntary pool for behavioral studies. Participants received 10 € reimbursement and provided written informed consent.

2.2 | Task

Action file binding was investigated using a previously established paradigm (Stoet & Hommel, 1999), also known as an R-R task (Colzato et al., 2006). The action file paradigm is shown in Figure 1.

The participants sat at a distance of 60 cm in front of a 17-in. CRT screen. During the trials, participants had to perform two tasks, task A and task B. Task B was embedded in task A. Stimuli were presented as white fonts on black screen background. Stimulus A was presented with the instruction not to react to it immediately, but only after presentation of stimulus B and the corresponding response B. Thus, task A had to be planned and withheld, while task B could be carried out immediately after presentation of stimulus B. The exact timing of the task was as follows. First, a fixation cross was displayed for 50 ms. Then, stimulus A appeared for 2,000 ms. Stimulus A consisted of a left- or right-pointing arrowhead and an asterisk either above or below the arrowhead. The arrowhead direction indicated whether the left or right hand was to be used for task A. The asterisk indicated the response direction. Next, the fixation cross was shown for another 50 ms, which was followed by stimulus B that was presented for 200 ms: it was either a symbol "&" indicating a left button press or a symbol "#" indicating a right button press. Once stimulus B was presented, participants had to perform task B followed by the already planned task A. Task A consisted of a sequence of three button presses. First, participants pressed the "home key" 4 or 6. This was indicated by the direction of the arrowhead in stimulus A. Second, the button above or below the home key had to be operated corresponding to the position of the asterisk in stimulus A. Third, the home key had to be pressed again. Thus, if stimulus A was a left-pointing arrowhead with an asterisk below it, the participants had to plan the following response sequence: 4 (left home key)—1 (position below)—4 (left home key). If stimulus A was a right-pointing arrowhead with an asterisk above it, the correct sequence was: 6 (right home key)—9 (position above)—6 (right home key). The combinations of the side of task A (left vs. right) and the side of task B (left vs. right) resulted in compatible (left–left or right–right) and incompatible (left–right or right–left) trials. Participants used keyboards to make their responses. The numerical pad on the right side of the keyboard was used: 1, 4, and 7 for left side responses, and 3, 6 and 9 for right side

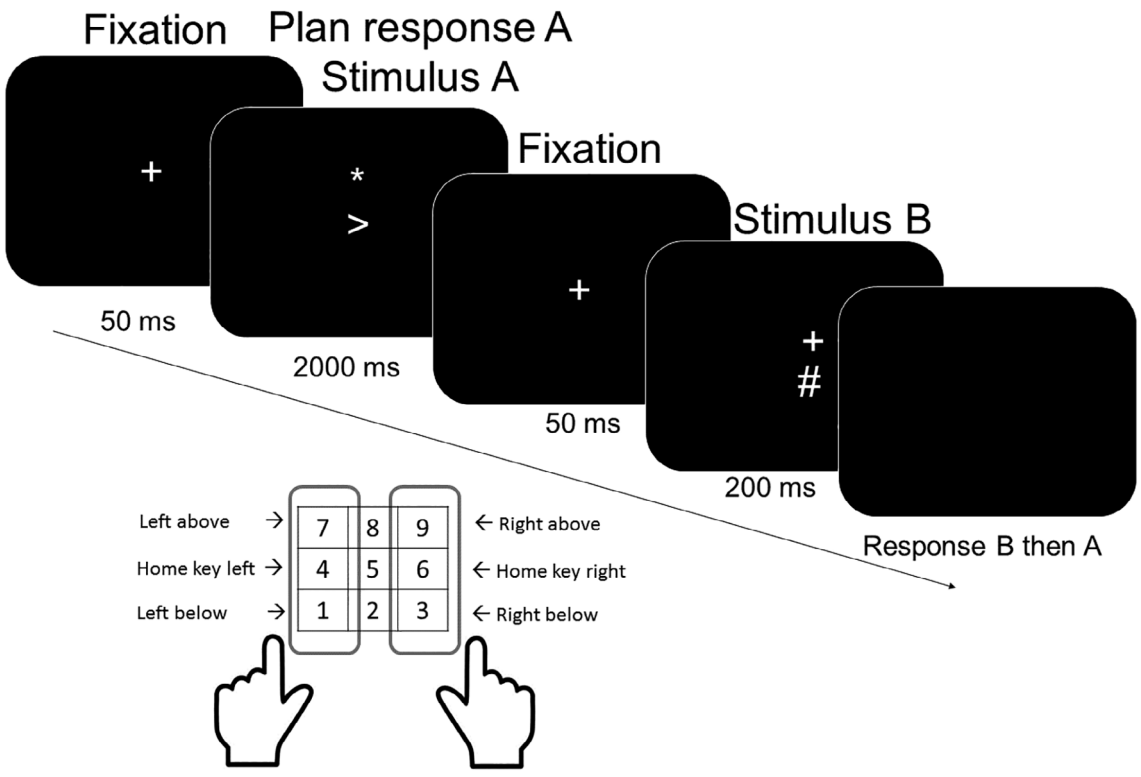

FIGURE 1 Schematic illustration of the paradigm. The figure represents the order of the stimuli during the trial including the timing of events. Below the timing information, the layout of the response buttons is displayed. Participants were required to use their left and right index fingers corresponding to the side of response

responses. Participants were instructed to use their left index finger on the left side of the pad, and their right index finger on the right side of the pad. Regarding the reaction times for response A, the first part of response A is measured from response B, the second part from the 1st part of response A, and the 3rd part is measures from the 2nd part of response A. After a practice of 40 trials, participants had to perform 256 trials during the experiment, in which half of them were compatible (overlap between response A and B) and half incompatible (no overlap between response A and response B). The possible mappings of task B were counterbalanced across participants.

2.3 | EEG recording and analysis

The EEG was recorded using 60 Ag/AgCl electrodes (500 Hz sampling rate; electrode impedance <5 kΩ) (EasyCap, Wörthsee, Germany) with equidistant cap layout. The signal was collected with a "QuickAmp" amplifier and the "Brain Vision Recorder" software (Brain Products, Gilching, Germany). Ground and reference electrodes were positioned at coordinates of θ = 58, φ = 78 and θ = 90, φ = 90. The latter one is corresponding to electrode position Fpz. Data pre-processing was conducted in Brain Vision Analyzer (Brain Products, Gilching, Germany). First, the recorded signal was down-sampled to 256 Hz and band-pass filter (IIR) was applied with 0.5 Hz to 20 Hz and an order of 8. Then, the data were re-referenced to the average activity of all electrodes. In the next step, the data was manually inspected to remove potential technical artifacts. Remaining, periodical artifacts (vertical and horizontal eye movements, blinks, pulse artifacts) were removed by an independent component analysis (ICA, Infomax algorithm). Components with identifiable spectrum and topography, such as vertical and horizontal eye movements, cardiovascular and muscle artifacts have been removed. The pre-processed, continuous data were segmented by using epochs locked either on stimulus B (−500 to 1,500 ms) or response B (−500 to 1,500 ms). Only trials with correct response B and response A were segmented. For all combinations of overlap levels (feature overlap vs. no feature overlap trials) and the response direction of the response B (left vs. right response), separate segments were generated. Thus, left feature overlap, left no feature overlap, right feature overlap and right no feature overlap segments were created both for stimulus- and response-locked segmentations. Differentiating between left- and right-sided responses in the EEG analysis was necessary due to the potential motor lateralization effects. Then, an automatic artifact rejection method was applied (time window: 500 ms before and 1,500 ms after the Stimulus B or Response B). In this step, all segments were discarded with amplitudes >150 μV, or <−150 μV, or activities <0.5 μV over a time interval of at least 100 ms. This threshold rejection was meant to remove any remaining larger artifact, such as saccade components or brief motor noise. After the artifact rejection, one participant was removed from the analysis due to insufficient number of kept segments. Then, a current source density (CSD) transformation was used (Kayser & Tenke, 2015; Perrin, Pernier, Bertrand, & Echallier, 1989) with four order of splines to generate reference-free data. The CSD transformation creates a spatial filter, which then highlights the scalp topography of neural activity. Thus, CSD transformation helps with identifying stimulus- or response-locked activities on individual electrodes (Nunez, Pilgreen, Westdorp, Law, & Nelson, 1991; Tenke & Kayser, 2012). Then, the segmented data were baseline corrected (time window: −300 ms to 0 ms prior Stimulus B onset). After the temporal decomposition (see Section 2.4) the baseline was adjusted to −500 ms to −300 ms prior to the onset of Stimulus B. Then, the data was averaged separately for each condition and participant. According to the hypotheses for the standard time-domain data analyses, especially the LRP was of interest. The LRP was calculated according to the definition by Coles (1989):

$$\frac{(\mathrm{ER}-\mathrm{EL})\ \text{left hand response} + (\mathrm{EL}-\mathrm{ER})\ \text{right hand response}}{2}$$

Where EL signifies the brain potential recorded over the left and ER over the right motor cortex. In the current study, the most commonly used channels, C3 and C4 (Coles, 1989) were used to calculate the LRPs. The original waveforms on the channels C3 and C4 are depicted in the Supporting Information. According to Coles' (Coles, 1989) definition, a negative deviation in the stimulus-locked LRP (s-LRP) indicates correct response activation, a positive deviation indicates incorrect response activation. After visual inspection of the s-LRP waveforms, we identified a negative deviation, which was then analyzed in the time window of 220 to 420 ms after the presentation of Stimulus B. A potential incorrect response activation was quantified preceding the correct response activation: that is, between 50 and 200 ms after the presentation of Stimulus B. Similarly, post-response processes were quantified in 500–1,000 ms after stimulus presentation. Please, note, that this time window proceeding the response B also overlaps with the response As. Amplitudes in all the analyzed time windows differed from zero (all p's < .032). After inspecting the response-locked LRP (r-LRP) waveform, we identified a negative deviation in the time window preceding the response B with 300 ms to investigate lateralized response preparation. Additionally, a positive deflection was observed 80–200 ms after the response onset. This post-movement reafferent potential was used to analyze the sensory feedback after motor execution (Di Russo, Pitzalis, Aprile, & Spinelli, 2005; Kornhuber & Deecke, 2016; Rauchbauer, Pfabigan, & Lamm, 2018). Within these intervals, the mean amplitude was quantified for each single subject. Furthermore, to examine the oscillatory neural activity potentially related to LRP activities, such as low and high mu (Freeman, Itthipuripat, & Aron, 2016; Kelly & O'Connell, 2013) we performed time-frequency decomposition analyses. The description of related Methods and Results are available in the Supporting Information.

2.4 | Residue iteration decomposition

Residue iteration decomposition (RIDE) is based on the assumption that different superimposed components with variable inter-component

delays can be differentiated within ERPs (Ouyang et al., 2015). The RIDE method decomposes the recorded single-trial ERPs into $N = 3$ component clusters with either static or variable latencies. The created components can be tied to various stages of information processing. RIDE uses an iterative temporal decomposition, which has been used with robust results before (Mückschel, Chmielewski, Ziemssen, & Beste, 2017; Wolff, Mückschel, & Beste, 2017). Decomposition was applied to each electrode separately. Since RIDE performs the decomposition irrespective of the scalp distributions (Ouyang et al., 2015), the CSD-transformation does not affect the decomposition. In the current study, RIDE was performed according to established procedures (Chmielewski, Mückschel, Ziemssen, & Beste, 2017; Verleger, Metzner, Ouyang, Śmigasiewicz, & Zhou, 2014) applying the RIDE toolbox (see manual at http://cns.hkbu.edu.hk/RIDE.htm) in Matlab (Mathworks, Inc., Massachusetts). Latency information of the stimulus and response onsets were used to generate the S ("stimulus") and R ("response") clusters. The C ("central") cluster's latency was estimated on a single-trial basis and iteratively improved. RIDE requires predefined time windows to extract the waveforms for each cluster (Ouyang, Schacht, Zhou, & Sommer, 2013). Each of these has to cover the range within each component is expected to occur (Ouyang et al., 2013; Ouyang et al., 2015). The following intervals were used: for the S-cluster, 200 ms before and until 700 ms after Stimulus B; for the R-cluster, 300 ms before and after the Response B; for the C-cluster, 150 ms to 800 ms after Stimulus B. Using the stimulus and response markers, RIDE applies an iterative decomposition. This procedure creates median waveforms. For the C-cluster estimation process, RIDE subtracts R and S from each trial and aligns the residual of all trials to the latency information of C. This creates the waveform for the C-cluster. The same procedure is repeated to generate the clusters of R and S. The whole process is iterated until the convergence of all components. A detailed description of the method is available in Ouyang et al. (2015). For the obtained RIDE clusters, we used the same amplitude extraction method as described above (Stürmer et al., 2013). s-LRPs were calculated separately for the C-, R-, and S-clusters. For the r-LRP, an R-cluster could not be obtained since the response occurred at the zero point of the segments. Moreover, stimulus presentation could precede the segment of the r-LRPs, thus calculating the S-cluster would have been unreliable. Thus, we analyzed RIDE clusters only for the s-LRPs and not for the r-LRPs. Please, note, that the R-cluster of the s-LRP captures response-related activities, and thus, it can be viewed as a decomposed equivalent of the r-LRP.

2.5 | Multivariate pattern analysis

We performed MVPA on the pre-processed and segmented, undecomposed EEG and also on the RIDE decomposed data using the ADAM toolbox (version 1.05, Fahrenfort et al., 2018) in Matlab (Mathworks). Before the MVPA, the EEG data was down-sampled offline to 55 Hz. A linear discriminant classifier was trained and tested on each time point by using five-fold cross-validation. That is, the classifier was trained on 80% of the data, and tested 20% of the data, repeating this process until all data chunks had been tested. The Area Under the ROC Curve (AUC) was used as a measure of classification accuracy. Larger area indicates more accurate classification performance (Fahrenfort et al., 2018). The final performance metric was computed by creating the average of five test folds. Two categories were used to train the classifier: feature overlap and no feature overlap. In the case of unbalanced trial numbers in the categories, the majority class was down-sampled to avoid skewed classification (Fahrenfort et al., 2018). The EEG amplitudes at individual electrode channels were used as classification features, creating 60 features in both stimulus classes. A backward decoding model (BDM) (Fahrenfort et al., 2018) was used for training and to computing metric on testing. Next, temporal generalization matrices were calculated by using cross-classification across time. In this step, the stability of the observed pattern (undecomposed EEG, or decomposed C-, R-, and S-cluster activity) was evaluated over time by training the model in one time point and testing its discrimination performance in the remaining time points. Cross-classification was repeated for every time point. As a result, classification performance above chance level outside the diagonal axis indicates sustained neural activity. Additionally, topographical maps were created based on classifier weights for the individual electrode channels. Statistical analyses for the MVPA, that is, group statistics and multiple corrections were performed in ADAM (Fahrenfort et al., 2018). Two-sided *t*-tests against chance level (AUC = .05) were performed for each time sample across subjects. Cluster-based permutation was used as a correction for multiple comparisons as implemented in the ADAM software package.

2.6 | Statistics

Statistical analyses were performed by using JASP 0.11.1 (JASP Team, 2019). Mean accuracy (percentage of correct responses) and means of RT data (for correct responses) were calculated for each participant and each condition. To examine action file binding, accuracy and RT data were analyzed in paired samples *t*-tests between the feature overlap and no feature overlap conditions. Similarly, EEG data was quantified as mean activity in the time windows of 50–200 ms (incorrect response activation of Task B); 220–420 ms (correct response activation of Task B); 500–1,000 ms (response activations of Task A) on the s-LRP channel. In the RIDE-decomposed data mean activity was quantified in the same time windows. To quantify the onset latency of the correct response activation, the fractional peak method was used. The onset of the component was marked at the time when 30 % of the peak amplitude in the time window of 220–420 ms after stimulus B onset was reached, retrospectively. EEG data was quantified as mean activity in the time windows of −300 ms to 0 ms before and 80 ms to 200 ms after the response B on the r-LRP channel. In the case of violation of normality, Wilcoxon's test was used. We report Cohen's *d* as effect size. The Bayes factor as BF_{10} is reported to quantify the evidence for the null hypothesis. In the Bayesian analyses, the default Cauchy prior was used with the scale of 0.707.

3 | RESULTS

3.1 | Behavioral data

Participants performed Response B faster in the no feature overlap (445.8 ms ± 25.9) than in the feature overlap condition (465.1 ms ± 25.7), (t[28] = 3.11, p = .004, d = .578, BF_{10} = 9.43). At the same time, responses for Response B did not differ in accuracy between feature overlap conditions (t[28] = 1.80, p = .083, d = .333, BF_{10} = 0.81). Participants'cumulated reaction time for "A" responses did not differ between feature overlap (755.0 ms ± 41.9) and no feature overlap (760.5 ms ± 41.6), (t[28] = 0.62, p = .541, d = .115, BF_{10} = 0.42). However, overall accuracy for "A" responses were better in no feature overlap (98.3% ± 2.1) than in feature overlap (97.2% ± 3.1), (Z = 87.5, p = .026, d = .501, BF_{10} = 2.24). Reaction time and accuracy data separately for the three consecutive "A" responses are available in Table 1.

3.2 | Neurophysiology

3.2.1 | Lateralized readiness potentials

The s-LRP waveform is shown in Figure 2a, and the r-LRP waveform is shown in Figure 3.

To examine neurophysiological correlates of the code occupation effect (i.e., s-LRPs), we analyzed the conditions no feature overlap and feature overlap in the following time windows after Stimulus B presentation: 50–200 ms (incorrect response activation of Task B); 220–420 ms (correct response activation of Task B); 500–1,000 ms (response activations of Task A). In the time window corresponding to the incorrect response activation (50–200 ms), the mean amplitude was larger in the feature overlap (2.95 $\mu V/m^2$ ± 2.2) than in the no feature overlap condition (–1.42 $\mu V/m^2$ ± 2.4), (t[28] = 6.10, p < .001, d = 1.154, BF_{10} > 999). In the time window corresponding to the correct response activation (220–420 ms), the mean amplitude was larger (more negative) in the no feature overlap (–9.00 $\mu V/m^2$ ± 1.4) than in the feature overlap condition (–3.15 $\mu V/m^2$ ± 0.9), (t[28] = 5.43, p < .001, d = 1.025, BF_{10} > 999). Moreover, the negative deflection in the no feature overlap condition (255.0 ms ± 11.1) had an earlier onset compared to the feature overlap condition (312.6 ms ± 9.2) (Z = 85.0, p = .007, d = 0.581, BF_{10} > 999). In the time window corresponding to the response activation of task A (500–1,000 ms) the mean amplitude was larger (more positive) in the no feature overlap (4.44 $\mu V/m^2$ ± 1.0) than in the feature overlap condition (–4.60 $\mu V/m^2$ ± 1.0), (t[28] = 5.43, p < .001, d = 0.984, BF_{10} > 999). Furthermore, we analyzed the code occupation effect on the r-LRP as a difference between the conditions of feature overlap and no feature overlap. In the time window of −300 ms prior to the Response B the conditions did not differ from each other (t[28] = 1.06, p = .299, d = 0.200, BF_{10} = 0.33). However, in the time window of 80 ms to 200 ms after the Response B, the positive deviation was larger in the no feature overlap (16.93 $\mu V/m^2$ ± 1.4) than in the feature overlap condition (–3.93 $\mu V/m^2$ ± 2.5), (t[28] = 6.87, p < .001, d = 1.347, BF_{10} > 999).

3.2.2 | Signal decomposition results

The waveforms of the s-LRP decomposed into the S-cluster, the C-cluster, and the R-cluster are shown in Figure 2b–d.

In the S-cluster, in the time window corresponding to the incorrect response activation (50–200 ms), the mean amplitude was larger in feature overlap (0.91 $\mu V/m^2$ ± 0.11) than in the no feature overlap condition (–0.34 $\mu V/m^2$ ± 0.11), (t[28] = 6.54, p < .001, d = 1.235, BF_{10} > 999). In the time window corresponding to the correct response activation (220–420 ms), the mean amplitude was larger (more negative) in no feature overlap (–0.95 $\mu V/m^2$ ± 0.2) than in the feature overlap condition (0.50 $\mu V/m^2$ ± 0.2), (t[28] = 7.18, p < .001, d = 1.357, BF_{10} > 999). However, the onset latencies between the no feature overlap and feature overlap conditions did not differ from each other (Z = 147.0, p = .477, d = 0.162, BF_{10} = 0.637). In the time window corresponding to the response activation of task A (500–1,000 ms) the mean amplitude did not differ from zero (t[28] = 1.39, p = .176, d = 0.263), therefore, it was not analyzed.

In the C-cluster, in the time window corresponding to the incorrect response activation (50–200 ms), the mean amplitude was more negative in feature overlap (–0.29 $\mu V/m^2$ ± 0.06) than in no feature overlap condition (–0.06 $\mu V/m^2$ ± .04), (t[28] = 3.29, p = .003, d = 0.622, BF_{10} = 13.834). In the time window corresponding to the correct response activation (220–420 ms), the mean amplitude did not differ between the conditions, (t[28] = 1.65, p = .111, d = 0.311,

TABLE 1 Accuracy and reaction time data of responses for task A and task B. RT for Response B is measured from Stimulus B presentation. Reaction times of the first Response A is measured from Response B, the second Response A is measured from the first Response A, and the third Response A is measured from the second Response A

	Feature overlap		No feature overlap		Feature overlap		No feature overlap	
	Accuracy (%)	*SE*	Accuracy (%)	SE	RT (ms)	*SE*	RT (ms)	*SE*
1st Response A	97.4	0.5	98.9	0.3	309	22.4	308.9	21.2
2nd Response A	96.5	0.7	97.8	0.5	228	12.9	233.8	13.1
3rd Response A	97.4	0.5	98.3	0.4	217.9	10.7	217.8	11.5
Response B	98.9	0.3	99.3	0.2	465.1	25.7	445.8	25.9

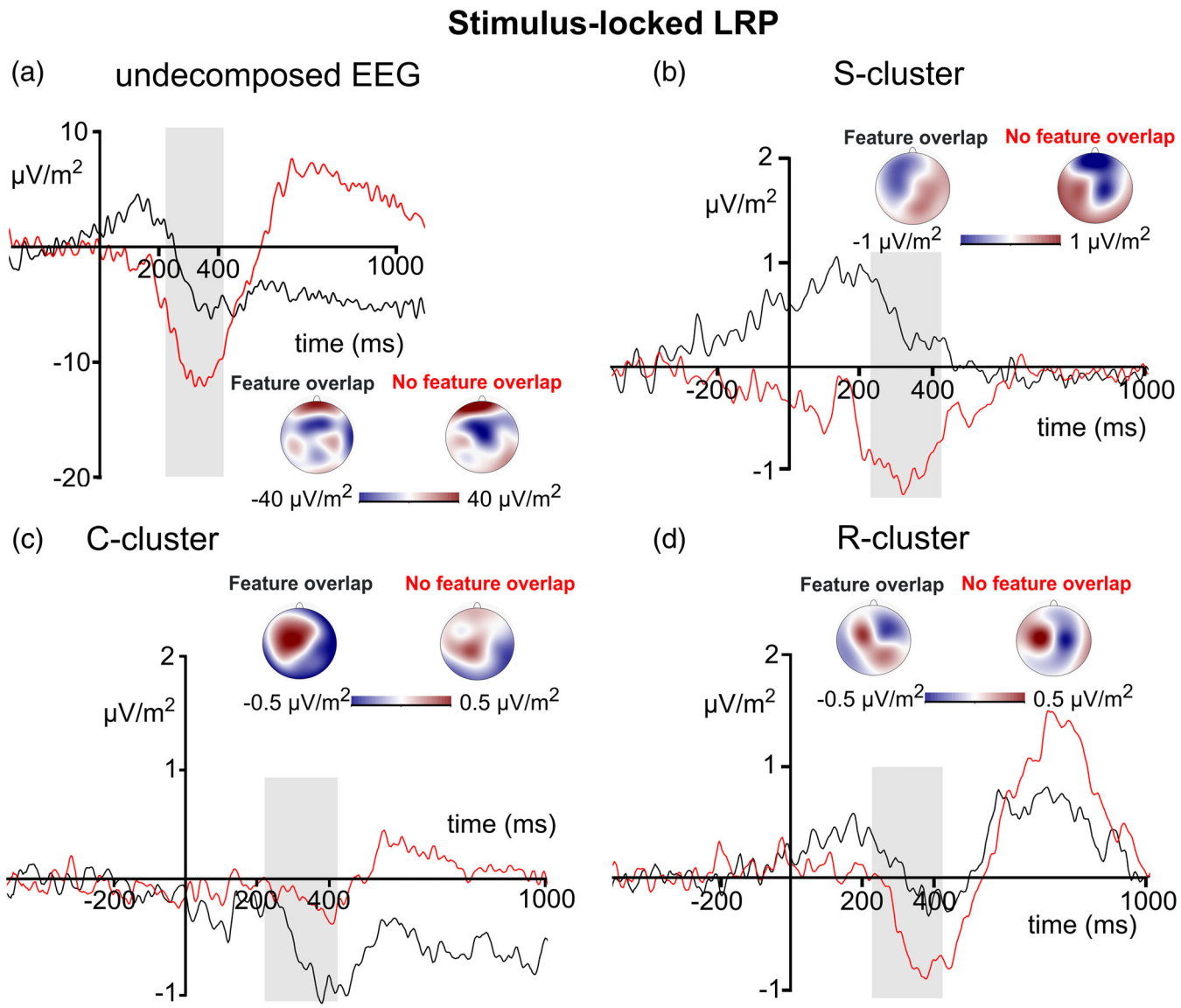

FIGURE 2 Stimulus-locked LRP waveforms. Time point zero denotes the stimulus presentation. S-LRPs are shown across two conditions: feature overlap in black, and no feature overlap in red. The analyzed time window of the correct response activation (220 ms to 420 ms) is marked with a shaded area. For the topography plots, difference waves were created between the contralateral and ipsilateral sides in the feature overlap and in the no feature overlap conditions, separately in the undecomposed EEG, and in the three RIDE clusters. The scalp topography plots show the distribution of the mean activity of the contralateral-ipsilateral difference waves of the time window of correct response activation. Panel (a) presents the standard ERP results. Panel (b) presents the s-LRP calculated from the decomposed S-cluster data. Panel (c) shows the s-LRP waveforms calculated from the decomposed C-cluster data. Panel (d) presents the s-LRP calculated from the decomposed R-cluster data. LRP, lateralized readiness potential

BF_{10} = 0.66). Similarly, the onset latencies between the no feature overlap and feature overlap conditions did not differ from each other (t[28] = 0.45, p = .657, d = 0.085, BF_{10} = 0.220). In the time window corresponding to the response activation of task A (500–1,000 ms) the mean amplitude was larger (more negative) in the feature overlap (–0.59 μV/m^2 ± 0.06) than in the no feature overlap condition (0.16 μV/m^2 ± 0.12), (t[28] = 4.99, p < .001, d = 0.942, BF_{10} > 999).

Visually, the time course of the R-cluster revealed strong similarities with the undecomposed s-LRP. In the R-cluster, in the time window corresponding to the incorrect response activation (50–200 ms), the mean amplitude was larger in feature overlap (0.40 μV/m^2 ± 0.07) than in no feature overlap condition (0.08 μV/m^2 ± 0.07), (Z = 345.0, p < .001, d = 0.670, BF_{10} = 9.1). In the time window corresponding to the correct response activation (220–420 ms), the mean amplitude was larger (more negative) in the no feature overlap (–0.56 μV/m^2 ± 0.1) than in the feature overlap condition (–0.30 μV/m^2 ± 0.1), (t[28] = 2.39, p = .024, d = 0.451, BF_{10} = 2.20). However, the onset latencies between the no feature overlap and feature overlap conditions did not differ from each other (Z = 261.0, p = .190, d = 0.286, BF_{10} = 0.320). In the time window corresponding to the response

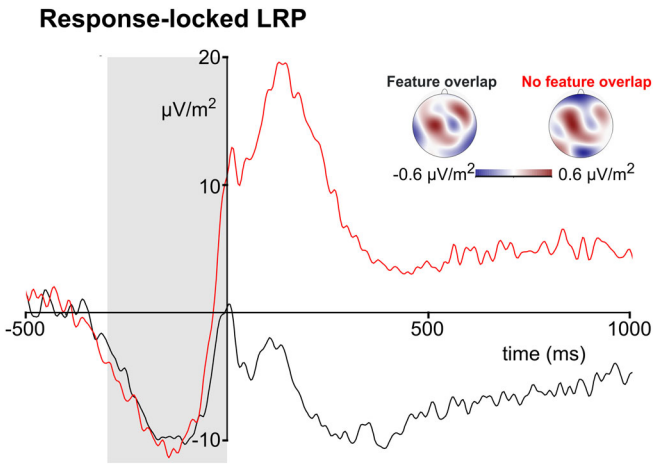

FIGURE 3 Response-locked LRP waveforms. Time point zero denotes the registration of the response. R-LRPs are shown across two conditions: feature overlap in black, and no feature overlap in red. The analyzed time window of the response activation (−300 ms to 0 ms) is marked with a shaded area. For the topography plots, difference waves were created between the contralateral and ipsilateral sides in the feature overlap and in the no feature overlap conditions. The scalp topography plots show the distribution of the mean activity of the contralateral-ipsilateral difference wave of the time window of the response activation (−300 ms to 0 ms). LRP, lateralized readiness potential

activation of task A (500–1,000 ms) the mean amplitude was larger (more positive) in the no feature overlap (0.71 $\mu V/m^2 \pm 0.13$) than in the feature overlap condition (0.45 $\mu V/m^2 \pm 0.09$), ($t[28] = 2.67$, $p = .013$, $d = 0.505$, $BF_{10} = 3.79$).

3.2.3 | Multivariate pattern analysis results

First, we present the decoding accuracy results on the performance of the classification. Next, we present the temporal generalization matrices on the stability of the action file representations. We provide this information separately for the undecomposed s-LRP, and for the decomposed s-LRP C-, R-, and S-cluster data. Decoding performance and temporal generalization results are depicted in Figure 4.

In the undecomposed EEG, significant differences ($p < .05$) were found between the classes of no feature overlap and feature overlap 150 ms to 200 ms after the presentation of stimulus B. Additionally, difference between classes was significant from 375 ms to 800 ms. In the C-cluster, the classification was significantly above chance for the whole length of the trial, with the exception of a time window between 250 ms and 300 ms. Similarly, in the R-cluster, significant differences occurred between feature overlap and no feature overlap classes in the whole trial length. Lastly, in the S-cluster, the classification performed above chance level for the entire length of the trial. Thus, both in the undecomposed and in the RIDE-decomposed data, the MVPA yielded successful classifications, suggesting that action file representations can be detected in the neurophysiological data.

Consequently, the temporal generalization matrix shows that in the undecomposed EEG a chain-like diagonal activation was detected after 400 ms of Stimulus B presentation. Additionally, a smaller cluster was detected significantly above chance level between 150 ms and 200 ms after Stimulus B onset. In the C-cluster, a jittered diagonal activity was detected from 200 ms to the end of the trial. This activation was characterized by the same chain-like pattern as in the undecomposed EEG matrix. In the R-cluster, the main activation was detected as a ramping, chain-like above-chance activity from 250 ms to the end of the trial. This activation was characterized by an increasing activity. The main activation was preceded by an above-chance activity which started pre-trial and ended 50 ms after the stimulus presentation. In the S-cluster, the main above-chance activity occurred as a diagonal, jittered cluster from 200 ms to 700 ms after the stimulus presentation. Within this activation, the stability of the neural code was largest between 400 ms and 600 ms after the stimulus B. Similar to the R-cluster data, a smaller activity was detected starting pre-trial and ending at the beginning of the trial. Moreover, a smaller, off-diagonal below-chance activity was detected in the time windows of 150 ms to 600 ms.

4 | DISCUSSION

In the current study, we delineate the neurophysiological correlates of action file binding processes using EEG methods. To this end, we applied standard time-domain analyses in combination with temporal signal decomposition methods and MVPA methods. The behavioral data revealed stable binding effects in action files replicating previous findings (Colzato et al., 2006; Stoet & Hommel, 1999), that is, RTs were longer when task B shared features with task A, compared to conditions where task B did not share features with task A. Thus, feature integration impairs performance when a planned and another to-be performed action share feature codes. This effect is in line with the notion of the code occupation cost (Stoet & Hommel, 1999) suggesting that the features defining an action have become integrated. Importantly, the interference between planning a response and execute a subsequent one supports the TEC (Hommel, 2019; Hommel et al., 2001), as this interference occurred through the shared features between the responses.

4.1 | Time-domain results

On a neurophysiological level, code occupation costs present in behavioral data were reflected in the LRP. Binding effects were revealed particularly in the s-LRP. The s-LRP was locked to the presentation of stimulus B. When calculating the s-LRP in two-alternative choice response tasks, negative deflections indicate the activation of the correct response, whereas deflections in a positive direction indicate the activation of the incorrect response (Beste et al., 2010; Bryce et al., 2011; Falkenstein et al., 2006; Gratton et al., 1992; Stürmer et al., 2002). In the context of the current task, a small positivity

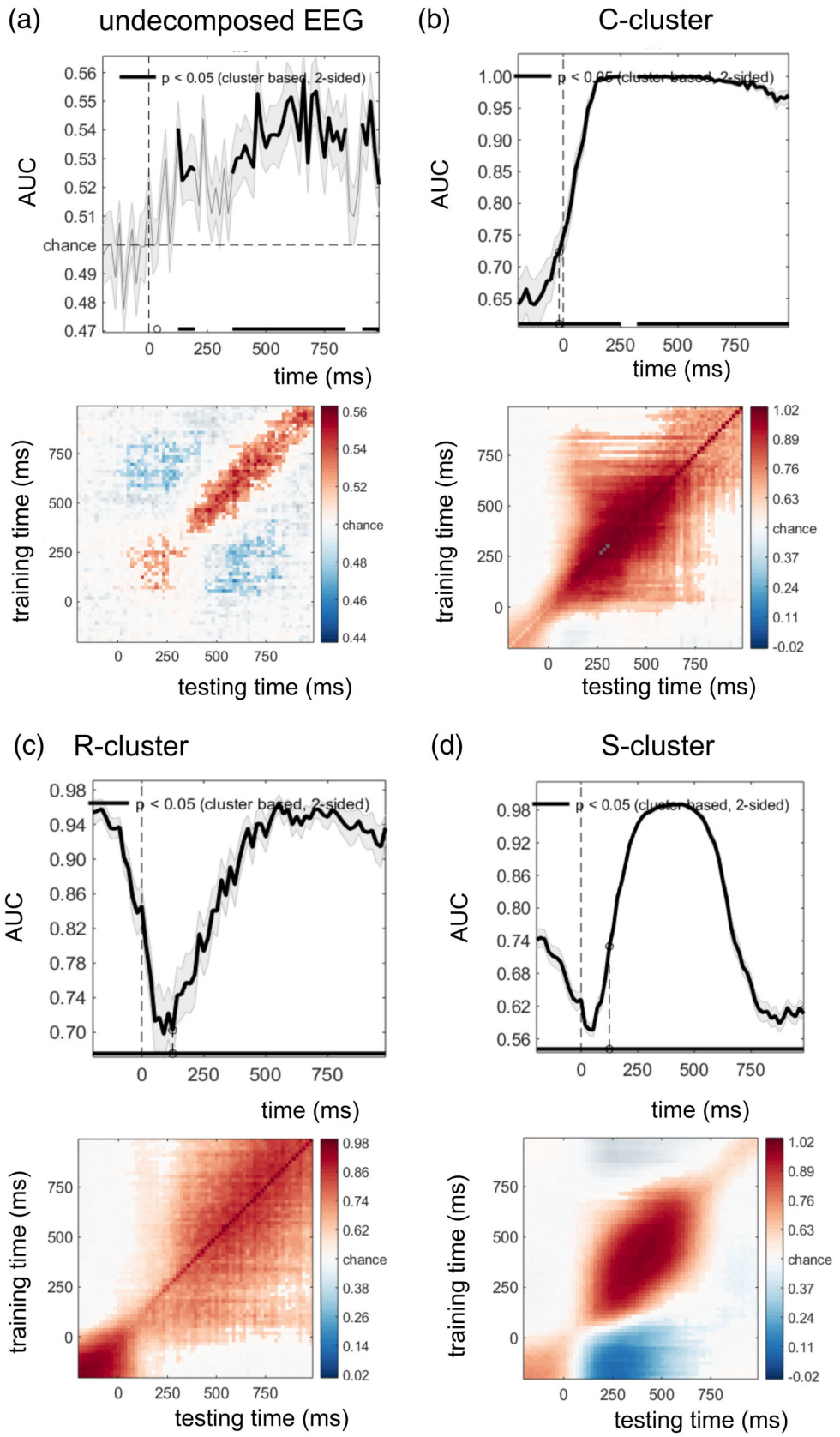

FIGURE 4 Decoding accuracy and temporal generalization matrix for the undecomposed EEG and the RIDE-clusters. Classification performances are shown across time between feature overlap and no feature overlap conditions. Significant time windows (p < .05, after cluster-based permutation) are indicated by thicker lines. Temporal generalization matrices show significant activations in saturated colors, while unsaturated colors represent p-values below the multiple-comparison corrected threshold

preceding the main negative deflection suggests an early automatic activation of a response code (Valt, Stürmer, Sommer, & Boehm, 2017). Specifically, the not-yet-required Response As can be implicated in the early positivity, and the Response B in the main negative activation of the s-LRP. Conversely, the behavioral data corresponds to this interpretation. When there was no feature overlap

between responses to stimulus A and to stimulus B, the RTs were ~445 ms, and the EEG data revealed earlier and larger negativity of the s-LRP around 400 ms after stimulus presentation compared to conditions with feature overlap, where RTs were slower (~465 ms).

It is likely that the s-LRP reflects pre-motor processes (Beste et al., 2009; Coles, 1989; Masaki et al., 2004; Osman et al., 1995; van der Lubbe et al., 2001; Wild-Wall et al., 2003). Thus, in line with the theoretical framework and our hypothesis, interference of action feature codes between task A and task B diminishes the efficiency of processes to prepare task B. It seems that activation of the different action-related features is slower and less efficient when there is an overlap between action features codes. Thus, the findings show that the cognitive concept of action feature binding can be directly mapped to neurophysiological measures of response activation processes. Importantly, in the condition with overlap between task A and task B action features, an early positive deflection of the curve was evident in the time window until 200 ms after stimulus B presentation. Since a positive deflection indicates the activation of a potentially competing (or incorrect) response, the data suggest that once task B is presented, action features of the not-yet-required response A become activated, in keeping with the cognitive concept of code occupation (Stoet & Hommel, 1999). Furthermore, following the negative peak at 400 ms after stimulus presentation the s-LRP then became positive when there was no feature overlap (as shown in Figure 2). This positivity was maximal around 600 ms to 700 ms after stimulus presentation. In the case of overlapping action feature codes between task A and B, no strong positive deflection was evident. To understand this, it is important to consider that after carrying out task B, participants immediately had to perform the three-step task A. The average RTs for response As are: ~309 ms, ~227 ms, and ~217 ms in the condition of action feature overlaps; and ~308 ms, ~233 ms, and ~217 ms in the condition of no action feature overlaps between task A and B. The first part of response A is measured from response B, the second part from the first part of response A, and the third part is measured from the second part of response A. Therefore, about 600 ms after stimulus B presentation, activations related to response A should become evident at the neurophysiological level. As mentioned, positive deflections in the s-LRP denote the activation of the incorrect response. Since the s-LRP was calculated based on the presentation of the task B stimulus, the observed positive deflection in the s-LRP in the case of no action feature overlaps between tasks A and B, reflects the activation of responses A, that was "incorrect" or "competing" with respect to the just completed task B. This neurophysiological data thus suggests that the pre-motor activation of task A after completion of task B is also affected by action feature overlaps between responses. The r-LRP data reflecting processes of motor execution (Beste et al., 2009; Coles, 1989; Masaki et al., 2004; Osman et al., 1995; van der Lubbe et al., 2001; Wild-Wall et al., 2003) corroborated that the findings on code occupation costs are very specific for the level of pre-motor activation processes mirrored in the s-LRP data. For the r-LRP, no differences in amplitude and/or onset latency were found.

It may be argued that the r-LRP of response B revealed strong differences between the condition with action feature overlaps and that with no action feature overlap shortly after the response was executed. In motor execution paradigms, this post-movement positive deviation has been described as a Reafferent Potential (RAP) and has been linked to sensory feedback of the executed action (Di Russo et al., 2005; Kornhuber & Deecke, 2016; Rauchbauer et al., 2018). It is conceivable, that sensorimotor information of the just performed action has a larger functional relevance when it is embedded in other responses with different action features. This post-response positivity, however, is likely to reflect overlapping activity with response activation of the A response. Thus, the current version of the paradigm does not allow to straightforwardly interpreting the response-locked post-movement activity. In sum, the LRP data suggest that code occupation and bindings between action features specifically modulate pre-motor processes (s-LRP) and not the motor execution process itself (r-LRP).

4.2 | Time-domain results (decomposed data)

Importantly, we also conducted a temporal decomposition of the s-LRP data (Stürmer et al., 2013) using RIDE (Ouyang et al., 2015). This is relevant because Stürmer et al. (2013) showed that also within the s-LRP, different subprocesses can be distinguished in choice response tasks and that particularly the S-cluster and the R-cluster in the s-LRP are modulated. Stürmer et al. (2013) suggested that modulations in the S-cluster may reflect priming-related processes of response activation, whereas the R-cluster reflects processes of instruction-related response selection. In contrast, the C-cluster LRP was not sensitive to response selection processes, and did not resemble a typical LRP component (Stürmer et al., 2013). Similarly, the current findings suggest that processes in s-LRP are reflected in two functionally and neurophysiological distinct activity clusters - the R-cluster and the S-cluster:

By and large, the time course shown in the R-cluster reflects the time course of the undecomposed s-LRP data: that is, after an initial negative deflection with a peak ~400 ms after the stimulus that was larger in the condition with no action feature overlap, a pronounced positivity ~700 ms was evident. As with the undecomposed s-LRP, this positivity was also larger when there was no action feature overlap between task A and B. This cascade of neurophysiological modulations is interpreted similarly as for the undecomposed s-LRP data. Yet, in light of the functional interpretation of the s-LRP R-cluster by Stürmer et al. (2013), the neurophysiological dynamics may reflect processes of voluntary/instruction-related response activation and selection processes. Interestingly, there was no significant positive deflection of the S-cluster potential in the time window around 700 ms after response B stimulus presentation (see also Figure 2b). This suggests that functionally different processes related to action feature binding are reflected by the S-cluster and R-cluster. At the same time, especially in the condition with overlap between task A and B action features, a positive deflection of the curve was evident

in the R-cluster. Since a positive deflection indicates the activation of the incorrect response (Beste et al., 2010; Bryce et al., 2011; Falkenstein et al., 2006; Gratton et al., 1992; Stürmer et al., 2002) the data suggest that once task B is presented, action features of the not-yet-required response A become activated. This nicely fits the cognitive concept of code occupation as a principle describing action feature integration (Stoet & Hommel, 1999). Because action features between task A and B overlap, an incorrect response for B is initially activated. Stürmer et al. (2013) suggested that the S-cluster reflects some form of involuntary or priming-related processes in response activation. Similar processes may underlie the effects when there are overlaps in action feature codes. In the current paradigm, this response priming process largely corresponds to the planning of response A. Thus, while the R-cluster, similarly to the undecomposed LRP reflects response activation and selection of response B, the S-cluster is sensitive to the other half of the task. This possibly explains why the feature overlap and no feature overlap conditions started to deviate from each other prior to the presentation of stimulus B (but after the baseline). Of note, the R-cluster s-LRP was sensitive to code occupation effect while the undecomposed r-LRP was not. This disparity may be counterintuitive given that the R-cluster is created based on the time interval around the response marker, thus, it should carry similar information on the task dynamics as the r-LRP. However, the two components are different in terms of variability. The iterative latency correction of RIDE made the R-cluster LRP less susceptible to trial-to-trial variability and consequent blurring effects than the trial averaged r-LRP (Ouyang & Zhou, 2020). This methodological difference makes the R-cluster data better suitable to detect changes between experimental conditions.

Conversely, no effects were seen related to Response B in the C-cluster. In the time windows corresponding to Response A, the two conditions differed from each other, however, these components could not be linked to traditional parts of the LRP. This pattern is in stark contrast with the recent temporal decomposition results of event file coding (Opitz et al., 2020; Takacs, Zink, et al., 2020). Both general stimulus–response binding (Takacs, Zink, et al., 2020) and distractor-response bindings (Opitz et al., 2020) were seen in the C-cluster as opposed to the S- and R-cluster. This is not surprising, considering that the paradigms used in these studies required translational processes between stimulus and response, and they did not rely on binding between action features. Moreover, as Stürmer et al. has already demonstrated, the decomposed s-LRP is only visible in the S- and R-clusters, the C-cluster does not seem to reflect motor preparation at all. In contrast, the current experiment operated on the level of motor programs; therefore, it was not expected to see binding effects in the C-cluster but in the R-cluster. The difference between the neurophysiological coding levels of event files and action files is in line with the behavioral findings of Colzato et al. (2006). In that study, stimulus–response binding and response–response bindings were uncorrelated, suggesting that integration of feature codes is not a unitary process, but different binding mechanisms may operate parallel. Altogether, the current and previous studies (Opitz et al., 2020; Takacs, Zink, et al., 2020) dovetailed our knowledge on the relationship between the different types of bindings and the temporally decomposed EEG data. A dissociation can be envisaged in which integration of object and action features are detectable in the C-cluster, while integration between action features are detectable in the R-cluster. It remains an open question whether binding of object features could be seen predominantly in the S-cluster.

4.3 | Multivariate pattern analysis results

In addition to extensive LRP analyses, we also conducted MVPA, in which we contrasted the conditions with action feature overlap between tasks A and B with those where there was no action feature overlap. This approach was based on a previous study (Takacs, Zink, et al., 2020) in which conditions with different levels of event file binding were contrasted, and thus, the representation of the event file binding processes could be studied. Unlike the LRP approach that is informative about the mental chronometry of response-related processes (Beste et al., 2010; Bryce et al., 2011; Falkenstein et al., 2006; Gratton et al., 1992), the temporal generalization analysis is sensitive to the stability of neural patterns (Fahrenfort et al., 2018; Grootswagers et al., 2016; King & Dehaene, 2014). That is, changes of mental representations can be decoded by using MVPA (King & Dehaene, 2014). In the current study, the MVPA contrast allowed us to investigate the generalization of action file binding. The MVPA was performed for the undecomposed, as well as for the decomposed data (see Figure 4). The results from the MVPA analysis suggest that there is a temporally sustained representation of action feature codes in the neurophysiological signal. Between 400 ms and 800 ms after stimulus presentation of task B, a temporally stable diagonal-shaped representation pattern was found in the undecomposed data. Such a diagonal MVPA coding pattern has been suggested to reflect a chain of representations (King & Dehaene, 2014). Since responses to task B were carried out between ~445 and 465 ms after stimulus presentation, and the instruction was to execute a chain of three tasks A responses immediately after finishing task B (which took about 750 ms altogether), the temporally sustained activation from 400 ms onwards very likely reflects the cascade (chain) of task A action feature activation and execution. Since the execution of task A comprises premotor response activation processes as well the motor execution it is plausible that temporally sustained and chained representations were found. However, for the RIDE cluster, and particularly so for the C-cluster and the R-cluster, not only diagonal activity was shown. For the R-cluster, sustained activity was present even before the presentation of task B at time point zero. Since task A was presented before response B this may well reflect task A representations. This sustained representation was not evident in the undecomposed data. A possible reason for this is that RIDE reduces intra-individual variability in the data (Ouyang et al., 2013), which may make it easier to detect temporally stable patterns of representations in the neural signal. Also, especially the R-cluster is said to reveal motor-related processes (Ouyang et al., 2015) and particularly in the R-cluster sustained pretrial activity was strong. In the undecomposed EEG data, different coding levels

are intermingled in the neural signal (Chmielewski et al., 2017; Mückschel et al., 2017), which is a possible reason why this sort of activity was not evident. Probably, it is a residual action feature representation from the A-response of the previous trial are reflected by this pretrial activation pattern in the R-cluster of the s-LRP. Notably, similar pre-stimulus intertrial activity was detected also in event file coding in the C-cluster and R-cluster data (Takacs, Zink, et al., 2020). Interestingly, in action file binding, for the R-cluster, but also for the C-cluster, extended off-diagonal (ramping) activity is shown (King & Dehaene, 2014). This ramping activity was more extended in the R-cluster than in the C-cluster and more steadily increased throughout the trial. The S-cluster did not show this extended ramping activity. This difference in the extended off-diagonal temporally generalized activity pattern can interpreted that particularly motor or movement-related codes become steadily activated throughout the trial. This fits to the structure and logic of the experimental paradigm, in which various actions have to be planned, and performed in a cascade. Thus, the temporal generalization analysis was able to track the representational time course of motor feature activity in action files. Moreover, the current study further delineated how different types of bindings are represented in the neural signal. While event files are characterized by a continuous, gradually strengthening activity (Takacs, Zink, et al., 2020), action files consists of chains of the motor features, and a ramping activity as the response is being executed. This provides an important evidence for the TEC (Hommel, 2019; Hommel et al., 2001). While the theory suggested that at the representational level, object files, action files, and event files can be distinguished from each other, up to date there was no direct evidence for the existence of different neural representations of the three file types. However, the difference between the temporal generalization of event files (Takacs, Zink, et al., 2020) and action files fills this gap, and suggest that different binding processes can lead to different representational patterns, such as action and event files.

4.4 | Comparison between time-domain and multivariate pattern analyses

When comparing the different levels of neurophysiological analyses, it is important to discuss how they complement our knowledge of the emergence and processing of event files. The dynamics of creating an action file, that is, the act of binding, was not directly investigated in the current study. Instead, the neurophysiological processes were described time-locked to the point when an action file feature was re-activated by the presentation of task B. Therefore, the LRP results reflect the chronometry of response processes as a consequence of the integration of action file features in response planning. It was revealed that this integration particularly affects pre-motor processes, and it can be detected primarily in the response level (R-cluster) and not in the stimulus (S-cluster) or stimulus–response translational (C-cluster) levels. That is, action files affected specific response-related processes at a specific coding level through code occupation between embedded tasks' responses. Thus, the phenomenon of code occupation and the existence of action file representations were confirmed in an indirect fashion, by the behavioral effects and the ERP correlates. In contrast, MVPA analyses showed that when action files are activated (in case of feature overlap), sustained neural activities were detected in the form of chains of motor features, and a ramping cluster. Thus, the temporal generalization provided more direct evidence for the existence of action files albeit without time-precision of the LRP analysis. The current results warrant further studies of how these action file representations emerge (i.e., close-up look at the binding process) and how do they integrate with the available pool of feature codes. For the latter question, the action file processes should be studied with different types of feature codes (Mocke, Weller, Frings, Rothermund, & Kunde, 2020). Importantly, temporal decomposition provided a more detailed picture of action file-related processes and action file representations per se, than the undecomposed EEG signal alone. In both cases, action file binding could be differentiated from previous results of event file binding mechanisms (Kleimaker et al., 2020; Opitz et al., 2020; Takacs, Mückschel, et al., 2020; Takacs, Zink, et al., 2020). This is in line with previous behavioral results suggesting the independence of action file binding and event file binding (Colzato et al., 2006). Thus, the combination of complementary neurophysiological methods were necessary to confirm that binding is not a unitary mechanism at the neural level.

5 | CONCLUSIONS

The present study addressed the neurophysiological mechanisms underlying binding processes in voluntary actions within the TEC framework. It examined the time course, functional different neural activity clusters, and the stability of the representational content of neurophysiological activity during action file coding. As such the study delineated the neurophysiological markers of the code occupation concept assumed to drive binding processes at the motor level (Stoet & Hommel, 1999). We showed that code occupation and bindings between action features specifically modulate pre-motor processes. Conversely, the motor execution processes were not modulated by action file binding. The temporal decomposition of the EEG signal further distinguished between action file related processes: the planned response, which the code occupation originated from, was reflected in general response selection (R-cluster) but not in priming-related (S-cluster) response activation. Altogether, the neurophysiological correlates of action file binding suggest that parallel, stimulus- and response-related pre-motor processes are responsible for the code occupation. Moreover, decoded EEG and temporally decomposed neural signal indicated that action files are represented as a continuous chain of activations. Within this chain, inhibitory and response re-activation patterns can be distinguished with signal decomposition.

ACKNOWLEDGMENT

Open access funding enabled and organized by Projekt DEAL. Open access funding enabled and organized by Projekt DEAL.

CONFLICT OF INTEREST

The authors declare no potential conflict of interest.

DATA AVAILABILITY STATEMENT

The data that support the findings of this study are available from the corresponding author upon reasonable request.

ETHICS STATEMENT

All participants provided written informed consent and received a financial reimbursement for their study participation. The ethics committee of the TU Dresden approved this study.

ORCID

Adam Takacs https://orcid.org/0000-0002-6575-727X
Christian Beste https://orcid.org/0000-0002-2989-9561

REFERENCES

Beste, C., Baune, B. T., Falkenstein, M., & Konrad, C. (2010). Variations in the TNF-α gene (TNF-α -308G→A) affect attention and action selection mechanisms in a dissociated fashion. *Journal of Neurophysiology*, *104*, 2523–2531.

Beste, C., Konrad, C., Saft, C., Ukas, T., Andrich, J., Pfleiderer, B., … Falkenstein, M. (2009). Alterations in voluntary movement execution in Huntington's disease are related to the dominant motor system: Evidence from event-related potentials. *Experimental Neurology*, *216*, 148–157.

Beste, C., Saft, C., Andrich, J., Gold, R., & Falkenstein, M. (2008). Stimulus-response compatibility in Huntington's disease: A cognitive-neurophysiological analysis. *Journal of Neurophysiology*, *99*, 1213–1223.

Bryce, D., Szűcs, D., Soltész, F., & Whitebread, D. (2011). The development of inhibitory control: An averaged and single-trial lateralized readiness potential study. *NeuroImage*, *57*, 671–685.

Carlson TA, Grootswagers T, Robinson AK (2019): An introduction to time-resolved decoding analysis for M/EEG. ArXiv190504820 Q-Bio. http://arxiv.org/abs/1905.04820.

Chmielewski, W. X., Mückschel, M., Ziemssen, T., & Beste, C. (2017). The norepinephrine system affects specific neurophysiological subprocesses in the modulation of inhibitory control by working memory demands. *Human Brain Mapping*, *38*, 68–81.

Coles, M. G. H. (1989). Modern mind-brain reading: Psychophysiology, physiology, and cognition. *Psychophysiology*, *26*, 251–269.

Colzato, L. S., Warrens, M. J., & Hommel, B. (2006). Priming and binding in and across perception and action: A correlational analysis of the internal structure of event files. *The Quarterly Journal of Experimental Psychology*, *59*, 1785–1804.

de Jong, R., Wierda, M., Mulder, G., & Mulder, L. J. (1988). Use of partial stimulus information in response processing. *Journal of Experimental Psychology. Human Perception and Performance*, *14*, 682–692.

Di Russo, F., Pitzalis, S., Aprile, T., & Spinelli, D. (2005). Effect of practice on brain activity: An investigation in top-level rifle shooters. *Medicine and Science in Sports and Exercise*, *37*, 1586–1593.

Dippel, G., & Beste, C. (2015). A causal role of the right inferior frontal cortex in implementing strategies for multi-component behaviour. *Nature Communications*, *6*, 6587.

Duncan, J. (2010). The multiple-demand (MD) system of the primate brain: Mental programs for intelligent behaviour. *Trends in Cognitive Sciences*, *14*, 172–179.

Fahrenfort, J. J., van Driel, J., van Gaal, S., & Olivers, C. N. L. (2018). From ERPs to MVPA Using the Amsterdam Decoding and Modeling Toolbox (ADAM). *Frontiers in Neuroscience*, *12*. https://doi.org/10.3389/fnins.2018.00368/full

Falkenstein, M., Willemssen, R., Hohnsbein, J., & Hielscher, H. (2006). Effects of stimulus-response compatibility in Parkinson's disease: A psychophysiological analysis. *Journal of Neural Transmission*, *113*, 1449–1462.

Freeman, S. M., Itthipuripat, S., & Aron, A. R. (2016). High working memory load increases intracortical inhibition in primary motor cortex and diminishes the motor affordance effect. *The Journal of Neuroscience*, *36*, 5544–5555.

Gratton, G., Coles, M. G., & Donchin, E. (1992). Optimizing the use of information: strategic control of activation of responses. *Journal of Experimental Psychology. General*, *121*, 480–506.

Gratton, G., Coles, M. G., Sirevaag, E. J., Eriksen, C. W., & Donchin, E. (1988). Pre- and poststimulus activation of response channels: A psychophysiological analysis. *Journal of Experimental Psychology. Human Perception and Performance*, *14*, 331–344.

Grootswagers, T., Wardle, S. G., & Carlson, T. A. (2016). Decoding dynamic brain patterns from evoked responses: A tutorial on multivariate pattern analysis applied to time series neuroimaging data. *Journal of Cognitive Neuroscience*, *29*, 677–697.

Henson, R. N., Eckstein, D., Waszak, F., Frings, C., & Horner, A. J. (2014). Stimulus-response bindings in priming. *Trends in Cognitive Sciences*, *18*, 376–384.

Hommel, B. (2004). Event files: Feature binding in and across perception and action. *Trends in Cognitive Sciences*, *8*, 494–500.

Hommel, B. (2009). Action control according to TEC (theory of event coding). *Psychological Research*, *73*, 512–526.

Hommel, B. (2019). Theory of event coding (TEC) V2.0: Representing and controlling perception and action. *Attention, Perception, & Psychophysics*, *81*, 2139–2154.

Hommel, B., Müsseler, J., Aschersleben, G., & Prinz, W. (2001). The Theory of Event Coding (TEC): A framework for perception and action planning. *The Behavioral and Brain Sciences*, *24*, 849–878 discussion 878-937.

Kayser, J., & Tenke, C. E. (2015). On the benefits of using surface Laplacian (Current Source Density) methodology in electrophysiology. *International Journal of Psychophysiology: Official Journal of International Organization Psychophysiology*, *97*, 171–173.

Keizer, A. W., Verment, R. S., & Hommel, B. (2010). Enhancing cognitive control through neurofeedback: A role of gamma-band activity in managing episodic retrieval. *NeuroImage*, *49*, 3404–3413.

Kelly, S. P., & O'Connell, R. G. (2013). Internal and external influences on the rate of sensory evidence accumulation in the human brain. *The Journal of Neuroscience*, *33*, 19434–19441.

King, J.-R., & Dehaene, S. (2014). Characterizing the dynamics of mental representations: the temporal generalization method. *Trends in Cognitive Sciences*, *18*, 203–210.

Kleimaker, M., Takacs, A., Conte, G., Onken, R., Verrel, J., Bäumer, T., … Münchau, A. (2020). Increased perception-action binding in Tourette syndrome. *Brain*, *143*, 1934–1945.

Kornhuber, H. H., & Deecke, L. (2016). Brain potential changes in voluntary and passive movements in humans: readiness potential and reafferent potentials. *Pflügers Archiv: European Journal of Physiology*, *468*, 1115–1124.

Kühn, S., Keizer, A. W., Colzato, L. S., Rombouts, S. A. R. B., & Hommel, B. (2011). The neural underpinnings of event-file management: Evidence for stimulus-induced activation of and competition among stimulus-response bindings. *Journal of Cognitive Neuroscience*, *23*, 896–904.

Leuthold, H., & Jentzsch, I. (2001). Neural correlates of advance movement preparation: A dipole source analysis approach. *Cognitive Brain Research*, *12*, 207–224.

Masaki, H., Wild-wall, N., Sangals, J., & Sommer, W. (2004). The functional locus of the lateralized readiness potential. *Psychophysiology*, *41*, 220–230.

Mocke, V., Weller, L., Frings, C., Rothermund, K., & Kunde, W. (2020). Task relevance determines binding of effect features in action planning.

Attention, Perception, & Psychophysics, *82*, 3811–3831. https://doi.org/10.3758/s13414-020-02123-x

Moeller, B., Pfister, R., Kunde, W., & Frings, C. (2019). Selective binding of stimulus, response, and effect features. *Psychonomic Bulletin & Review*, *26*, 1627–1632.

Mückschel, M., Chmielewski, W., Ziemssen, T., & Beste, C. (2017). The norepinephrine system shows information-content specific properties during cognitive control—Evidence from EEG and pupillary responses. *NeuroImage*, *149*, 44–52.

Nunez, P. L., Pilgreen, K. L., Westdorp, A. F., Law, S. K., & Nelson, A. V. (1991). A Visual study of surface potentials and Laplacians due to distributed neocortical sources: Computer simulations and evoked potentials. *Brain Topography*, *4*, 151–168.

Opitz, A., Beste, C., & Stock, A.-K. (2020). Using temporal EEG signal decomposition to identify specific neurophysiological correlates of distractor-response bindings proposed by the theory of event coding. *NeuroImage*, *209*, 116524.

Osman, A., Moore, C. M., & Ulrich, R. (1995). Bisecting RT with lateralized readiness potentials: Precue effects after LRP onset. *Acta Psychologica*, *90*, 111–127.

Ouyang, G., Herzmann, G., Zhou, C., & Sommer, W. (2011). Residue iteration decomposition (RIDE): A new method to separate ERP components on the basis of latency variability in single trials. *Psychophysiology*, *48*, 1631–1647.

Ouyang, G., Schacht, A., Zhou, C., & Sommer, W. (2013). Overcoming limitations of the ERP method with residue iteration decomposition (RIDE): A demonstration in go/no-go experiments. *Psychophysiology*, *50*, 253–265.

Ouyang, G., Sommer, W., & Zhou, C. (2015). A toolbox for residue iteration decomposition (RIDE)—A method for the decomposition, reconstruction, and single trial analysis of event related potentials. *Journal of Neuroscience Methods*, *250*, 7–21.

Ouyang, G., & Zhou, C. (2020). Characterizing the brain's dynamical response from scalp-level neural electrical signals: A review of methodology development. *Cognitive Neurodynamics*, *14*, 731–742. https://doi.org/10.1007/s11571-020-09631-4

Perrin, F., Pernier, J., Bertrand, O., & Echallier, J. F. (1989). Spherical splines for scalp potential and current density mapping. *Electroencephalography and Clinical Neurophysiology*, *72*, 184–187.

Petruo, V. A., Stock, A.-K., Münchau, A., & Beste, C. (2016). A systems neurophysiology approach to voluntary event coding. *NeuroImage*, *135*, 324–332.

Rauchbauer, B., Pfabigan, D. M., & Lamm, C. (2018). Event-related potentials of automatic imitation are modulated by ethnicity during stimulus processing, but not during motor execution. *Scientific Reports*, *8*, 12760.

Stoet, G., & Hommel, B. (1999). Action planning and the temporal binding of response codes. *Journal of Experimental Psychology. Human Perception and Performance*, *25*, 1625–1640.

Stürmer, B., Leuthold, H., Soetens, E., Schröter, H., & Sommer, W. (2002). Control over location-based response activation in the Simon task: behavioral and electrophysiological evidence. *Journal of Experimental Psychology. Human Perception and Performance*, *28*, 1345–1363.

Stürmer, B., Ouyang, G., Zhou, C., Boldt, A., & Sommer, W. (2013). Separating stimulus-driven and response-related LRP components with residue iteration decomposition (RIDE): LRP component separation by RIDE. *Psychophysiology*, *50*, 70–73.

Takacs, A., Mückschel, M., Roessner, V., & Beste, C. (2020). Decoding stimulus-response representations and their stability using EEG-based multivariate pattern analysis. *Cerebral Cortex Communications*. https://doi.org/10.1093/texcom/tgaa016/5831171

Takacs, A., Zink, N., Wolff, N., Münchau, A., Mückschel, M., & Beste, C. (2020). Connecting EEG signal decomposition and response selection processes using the theory of event coding framework. *Human Brain Mapping*, *41*, 2862–2877.

Tenke, C. E., & Kayser, J. (2012). Generator localization by current source density (CSD): Implications of volume conduction and field closure at intracranial and scalp resolutions. *Clinical Neurophysiology*, *123*, 2328–2345.

Treisman, A. (1996). The binding problem. *Current Opinion in Neurobiology*, *6*, 171–178.

Treisman, A., & Kahneman, D. (1984). Changing views of attention and automaticity. In R. Parasuraman & D.R. Davis (Eds.) *Varieties of attention* (pp. 29–61). Orlando, FL: Academic Press.

Valt, C., Stürmer, B., Sommer, W., & Boehm, S. (2017). Early response activation in repetition priming: An LRP study. *Experimental Brain Research*, *235*, 2927–2934.

van der Lubbe, R. H. J., Jaśkowski, P., Wauschkuhn, B., & Verleger, R. (2001). Influence of time pressure in a simple response task, a choice-by-location task, and the Simon task. *Journal of Psychophysiology*, *15*, 241–255.

Verleger, R., Metzner, M. F., Ouyang, G., Śmigasiewicz, K., & Zhou, C. (2014). Testing the stimulus-to-response bridging function of the oddball-P3 by delayed response signals and residue iteration decomposition (RIDE). *NeuroImage*, *100*, 271–280.

Wild-Wall, N., Sangals, J., Sommer, W., & Leuthold, H. (2003). Are fingers special? Evidence about movement preparation from event-related brain potentials. *Psychophysiology*, *40*, 7–16.

Wolff, N., Mückschel, M., & Beste, C. (2017). Neural mechanisms and functional neuroanatomical networks during memory and cue-based task switching as revealed by residue iteration decomposition (RIDE) based source localization. *Brain Structure & Function*, *222*, 3819–3831.

Zhang, R., Schrempf, W., Brandt, M. D., Mückschel, M., Beste, C., & Stock, A.-K. (2018). RLS patients show better nocturnal performance in the Simon task due to diminished visuo-motor priming. *Clinical Neurophysiology: Official Journal of International Federation of Clinical Neurophysiology*, *129*, 112–121.

SUPPORTING INFORMATION

Additional supporting information may be found online in the Supporting Information section at the end of this article.

How to cite this article: Takacs A, Bluschke A, Kleimaker M, Münchau A, Beste C. Neurophysiological mechanisms underlying motor feature binding processes and representations. *Hum Brain Mapp*. 2021;42:1313–1327. https://doi.org/10.1002/hbm.25295